

# Beam asymmetry $\Sigma$ of $\eta'$ photoproduction off the proton at GRAAL

G. Mandaglio  
on behalf of the GRAAL collaboration

*Centro Siciliano di Fisica Nucleare e Struttura della Materia - Catania  
Department of Physics and Earth Sciences – University of Messina  
INFN Sezione di Catania*

LHPMF2013 – Messina – October 14<sup>th</sup> 2013

# Summary

-  Recent results and motivation
-  Graal experiment setup
-  Analysis of data
-  Results
-  Conclusions

# Recent $\eta'$ data off the proton

the threshold energy for  $\gamma + p \rightarrow \eta' + p$  is  $E_\gamma = 1.447$  GeV

“ $\gamma p \rightarrow \eta' p$  isolates  $I = 1/2$  resonances, thereby providing an “isospin filter” for the spectrum of broad, overlapping nucleon resonances”

the reaction was measured

at CLAS (2006 and 2009) from thr. up to 2.84 GeV by looking at



at CB-ELSA(2009) from thr. up to 2.55 GeV by looking at



Both experiment have been measured differential (total cross sections CBELSA only) but no polarization observables

# CLAS Results

PRL 96, 062001 (2006)

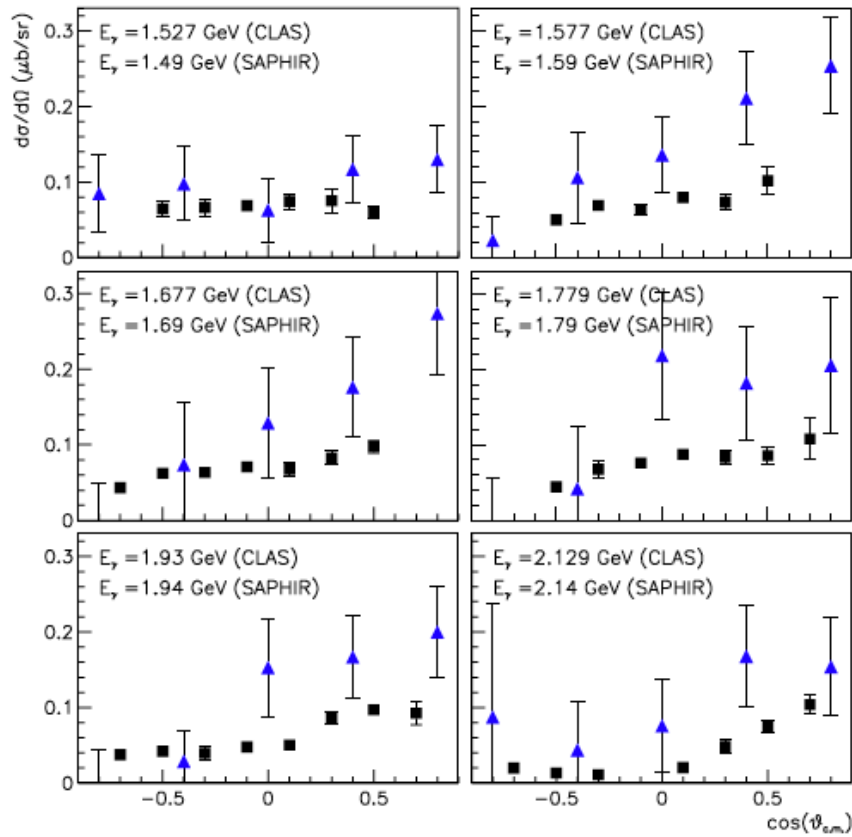


FIG. 2 (color online). Differential cross sections for  $\eta'$  photoproduction on the proton (black squares). Other results from SAPHIR [4] (blue triangles) are shown for comparison. Error bars shown include systematic and statistical uncertainties.

PHYSICAL REVIEW C 80, 045213 (2009)

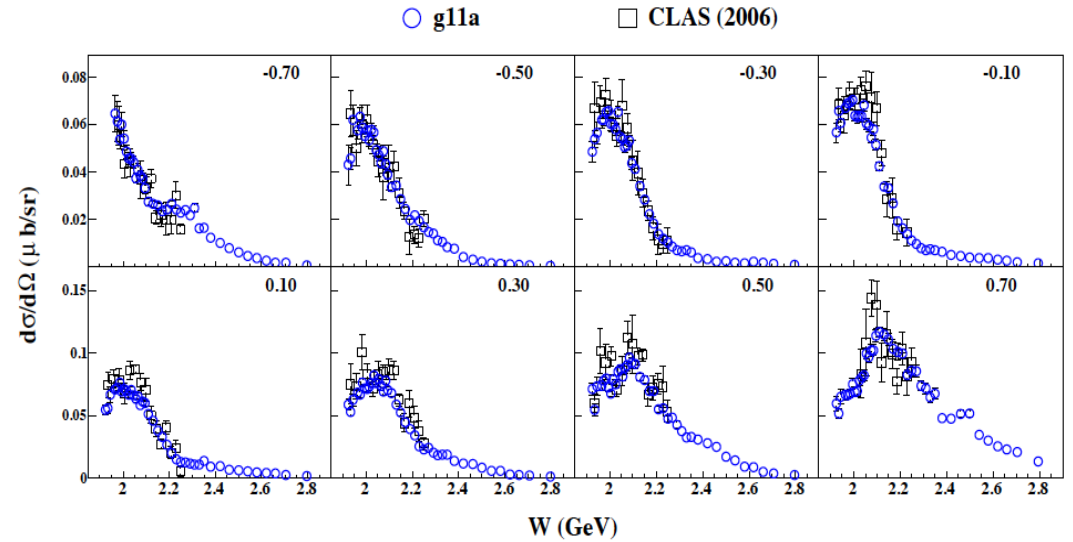


FIG. 9: (Color Online)  $\frac{d\sigma}{d\Omega}(\mu\text{b/sr})$  vs.  $W$  (GeV) for the  $\gamma p \rightarrow p\eta'$  reaction, in  $\cos\theta_{c.m.}^{\eta'}$  bins, from previous CLAS data [5] (open squares) and this work (blue open circles). For this comparison, our results were merged into 10  $\cos\theta_{c.m.}^{\eta'}$  bins, eight of which exactly overlap the earlier CLAS measurements shown here (see text for details). The centroid in  $\cos\theta_{c.m.}^{\eta'}$  of each bin is labeled on the plot.

An analysis of the data with **two different models of the process suggests for the first time Contributions from both the S(1535) and P(1710) nucleon resonances**

To the  $\eta N$  channel in photoproduction, the two Resonances previously identified as strongly coupling to the N channel [14].

# CB-ELSA

PHYSICAL REVIEW C 80, 055202 (2009)

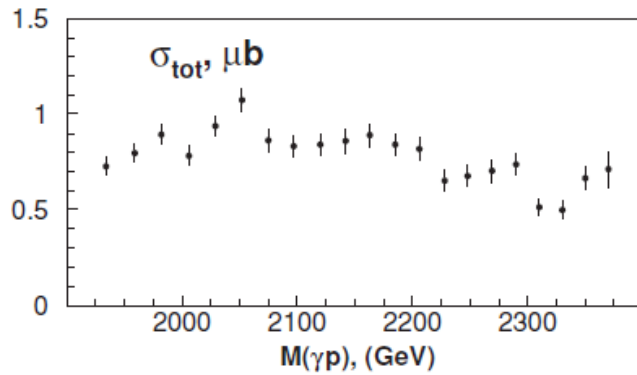


FIG. 15. Total  $\gamma p \rightarrow p\eta'$  cross section. The data points ( $\bullet$ ) are calculated by summation of the differential cross section.

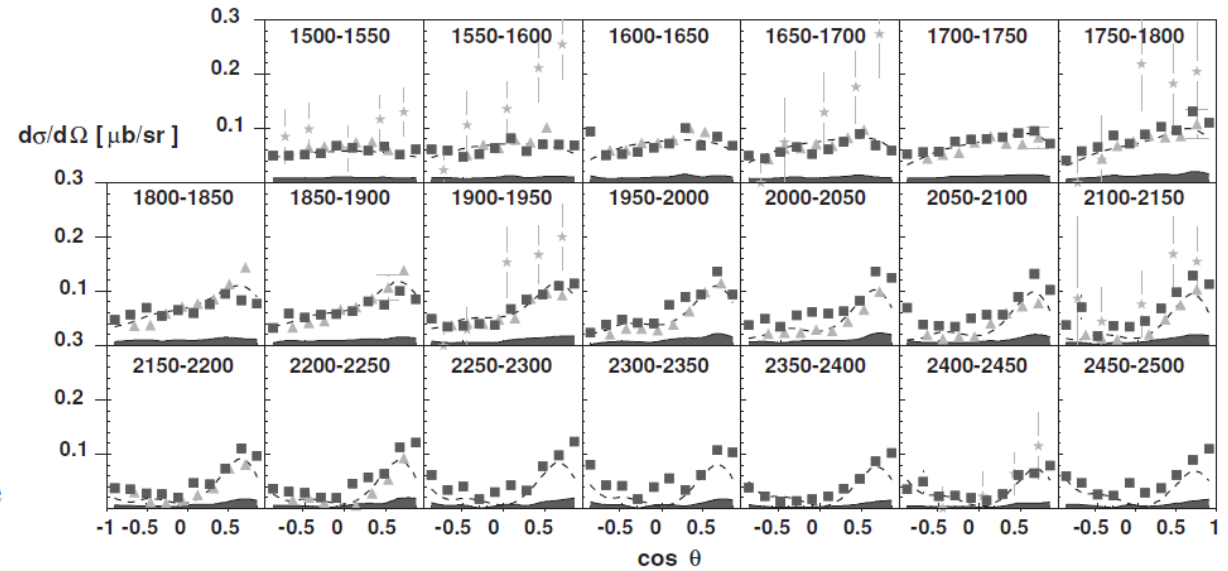


FIG. 10. Differential cross sections for the reaction  $\gamma p \rightarrow p\eta'$  (analyzed decay mode  $\eta' \rightarrow 2\pi^0\eta \rightarrow p6\gamma$ ) ( $\blacksquare$ ) using 50-MeV-wide energy bins and  $\cos \theta_{\text{c.m.}}^{\eta'}$  bins of width 0.2. The data cover the full angular range; energies are given in MeV. For comparison, data are shown from SAPHIR [28] ( $\star$ ) and CLAS [29] ( $\blacktriangle$ ). The SAPHIR data are based on only 250 events and, thus, have large error bars. The dashed line represents the SAID model [40].

Although limited in statistics, **all angular distributions appear to be flat indicating s-wave behavior of the reaction at the threshold.**

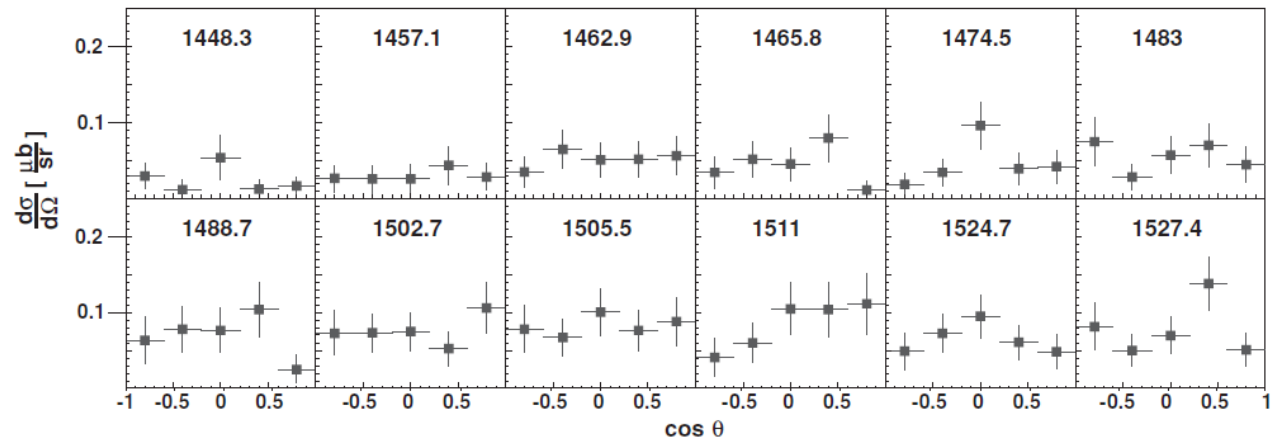


FIG. 11. Differential cross sections for the reaction  $\gamma p \rightarrow p\eta'$  close to the reaction threshold ( $\blacksquare$ ) determined for individual tagger channels using 5  $\cos \theta_{\text{c.m.}}^{\eta'}$  bins of width 0.4. Energies in the plots are given in MeV. Although limited in statistics, all angular distributions appear to be flat indicating  $s$ -wave behavior of the reaction at the threshold.

# Theory

Nakayama and Haberzettl

## relativistic meson-exchange model of hadronic interactions

Phys. Rev. C 73, 045211 (2006)

*$S_{11}$   $P_{11}$   $P_{13}$   $D_{13}$  and  $t$ -channel mesonic currents. The observed angular distribution is due to the interference between the  $t$ -channel and the nucleon  $s$ - and  $u$ -channel resonance contributions. The  $j = 3/2$  resonances are required to reproduce some of the details of the measured angular distribution.*

*“We emphasize, however, that cross-section data alone are unable to pin down the resonance parameters and it is shown that the beam and/or target asymmetries impose more stringent constraints on the parameter values.”*

Wen-Tai Chiang, Shin Nan Yang, Tiator, Vanderhaeghen, Drechsel  
**reggeized model for  $\eta$  and  $\eta'$  photoproduction on the nucleon**

*$S_{11}$   $P_{11}$   $P_{13}$   $D_{13}$  and  $t$ -channel vector meson exchanges described in terms of Regge trajectories to comply with the correct high energy behavior.*

*In the case of  $\eta'$  photoproduction, the threshold is too high to allow an acceptable description with vector meson poles in the  $t$ -channel. Unlike the case of  $\eta$  photoproduction, the use of Regge trajectories is able to improve the data description.*

*“In the case of  $\eta'$  production, polarization data, e.g. beam asymmetry could be very helpful to better determine the partial wave contributions in this reaction.”*

pseudo-scalar meson photoproduction is described by 4 complex helicity amplitudes

Nakayama and Haberzettl

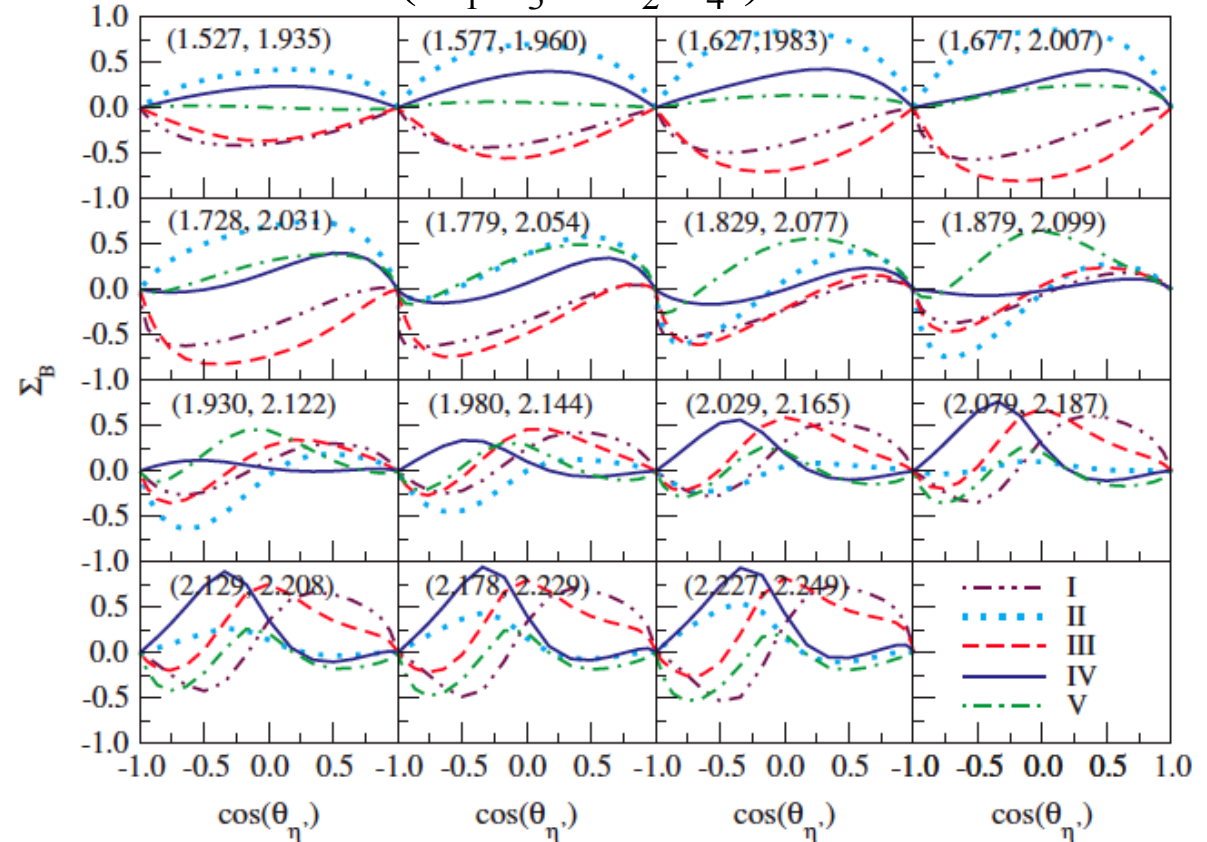
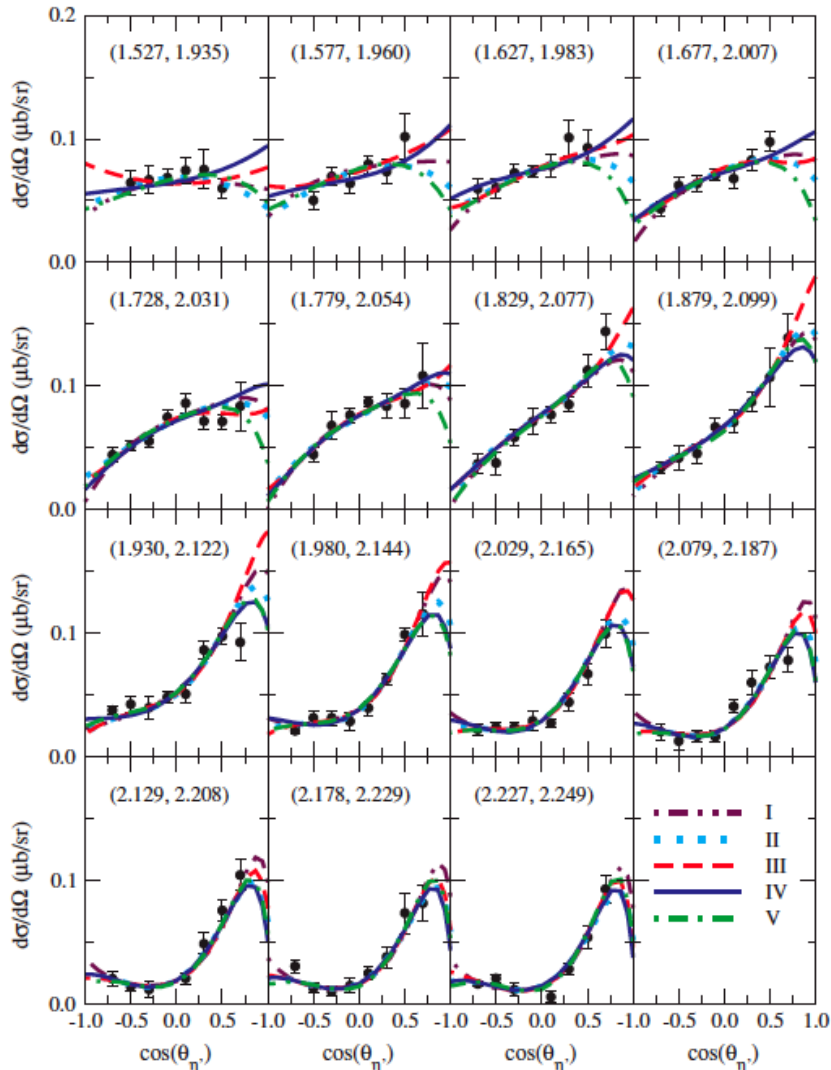
Phys. Rev. C 73, 045211 (2006)

$$d\sigma/d\Omega \sim H_1^2 + H_2^2 + H_3^2 + H_4^2$$

$$\Sigma \sim \text{Re} (H_1 H_4^* - H_2 H_3^*)$$

$$T \sim \text{Im} (H_1 H_2^* - H_3 H_4^*)$$

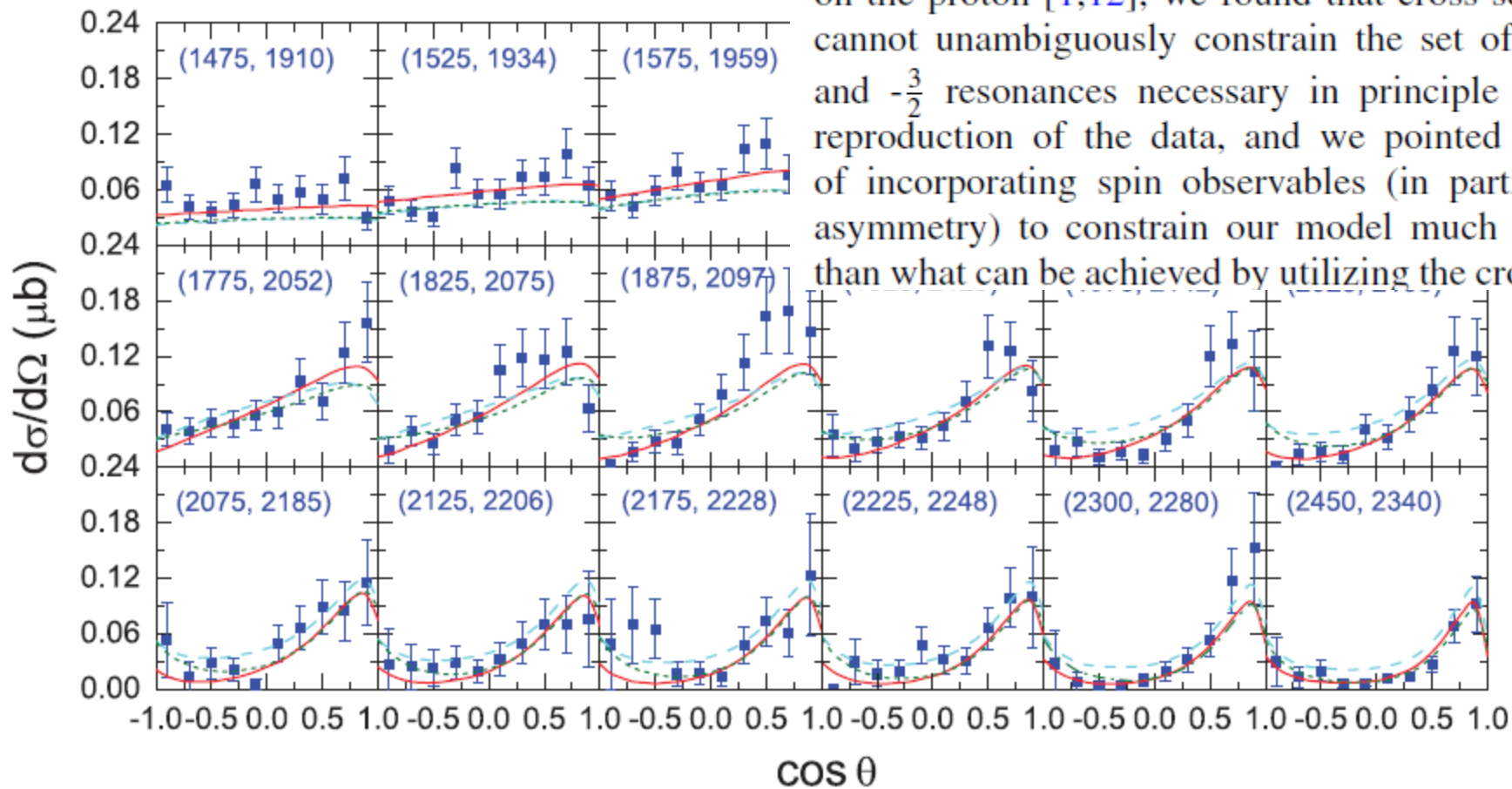
$$P \sim \text{Re} (H_1 H_3^* - H_2 H_4^*)$$



# Combined analysis of $\eta'$ production reactions: $\gamma N \rightarrow \eta' N$ , $NN \rightarrow NN\eta'$ , and $\pi N \rightarrow \eta' N$

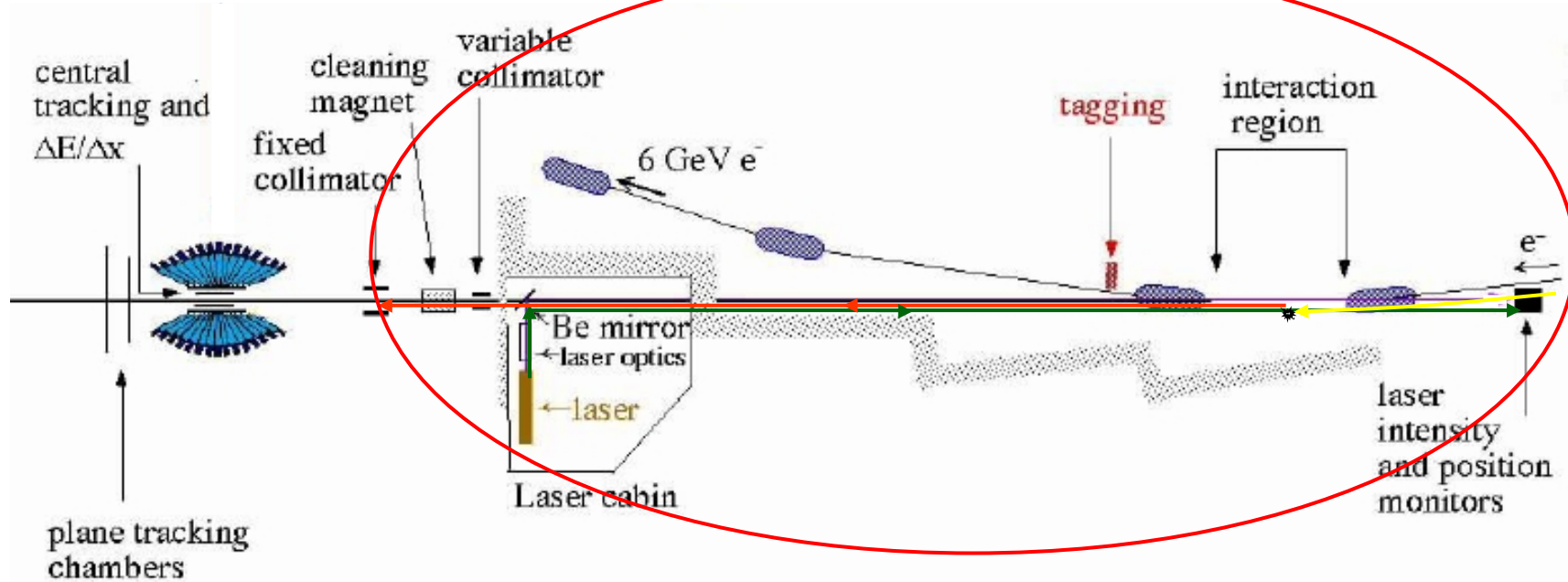
F. Huang,<sup>1,\*</sup> H. Haberzettl,<sup>2,†</sup> and K. Nakayama<sup>1,3,‡</sup>

To date, although there are ongoing efforts to measure the beam asymmetry [13] and the beam-target asymmetry [14], experimental data for spin observables are not available yet for  $\eta'$  production reactions. However, as we shall show in this



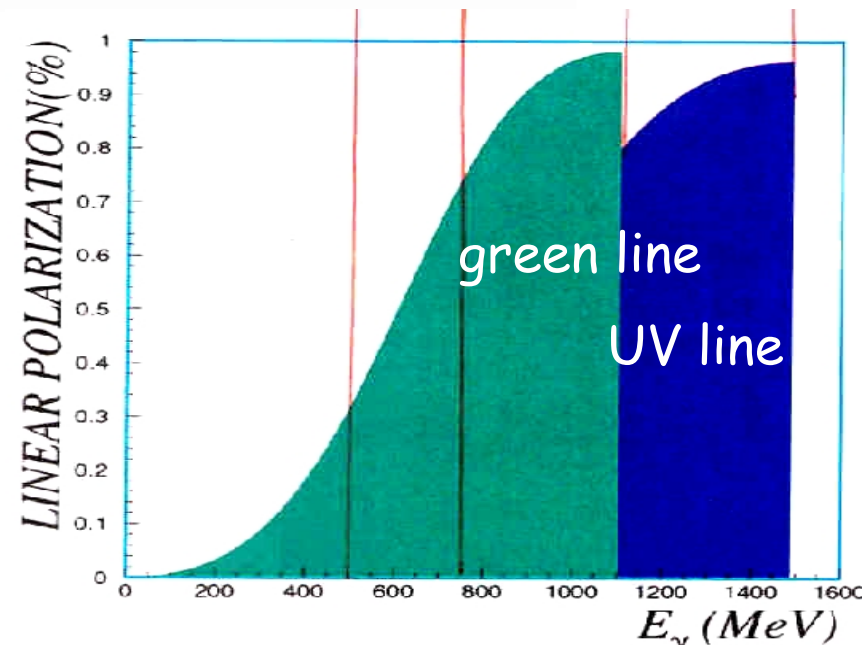
on the proton [1,12], we found that cross-section data alone cannot unambiguously constrain the set of minimal spin- $\frac{1}{2}$  and  $-\frac{3}{2}$  resonances necessary in principle for an adequate reproduction of the data, and we pointed to the necessity of incorporating spin observables (in particular, the beam asymmetry) to constrain our model much more stringently than what can be achieved by utilizing the cross section alone.

# GRAAL $\vec{\gamma}$ BEAM FEATURES



Compton scattering laser and ESRF storage ring electron ( $E_e = 6.04$  GeV)

- Energy resolution (16 MeV FWHM)
- Intensity  $\Phi_{\text{tag}} \sim 10^6 \gamma/s$
- Degree of polarization calculated by QED- close 100% at  $E_\gamma$  maximum

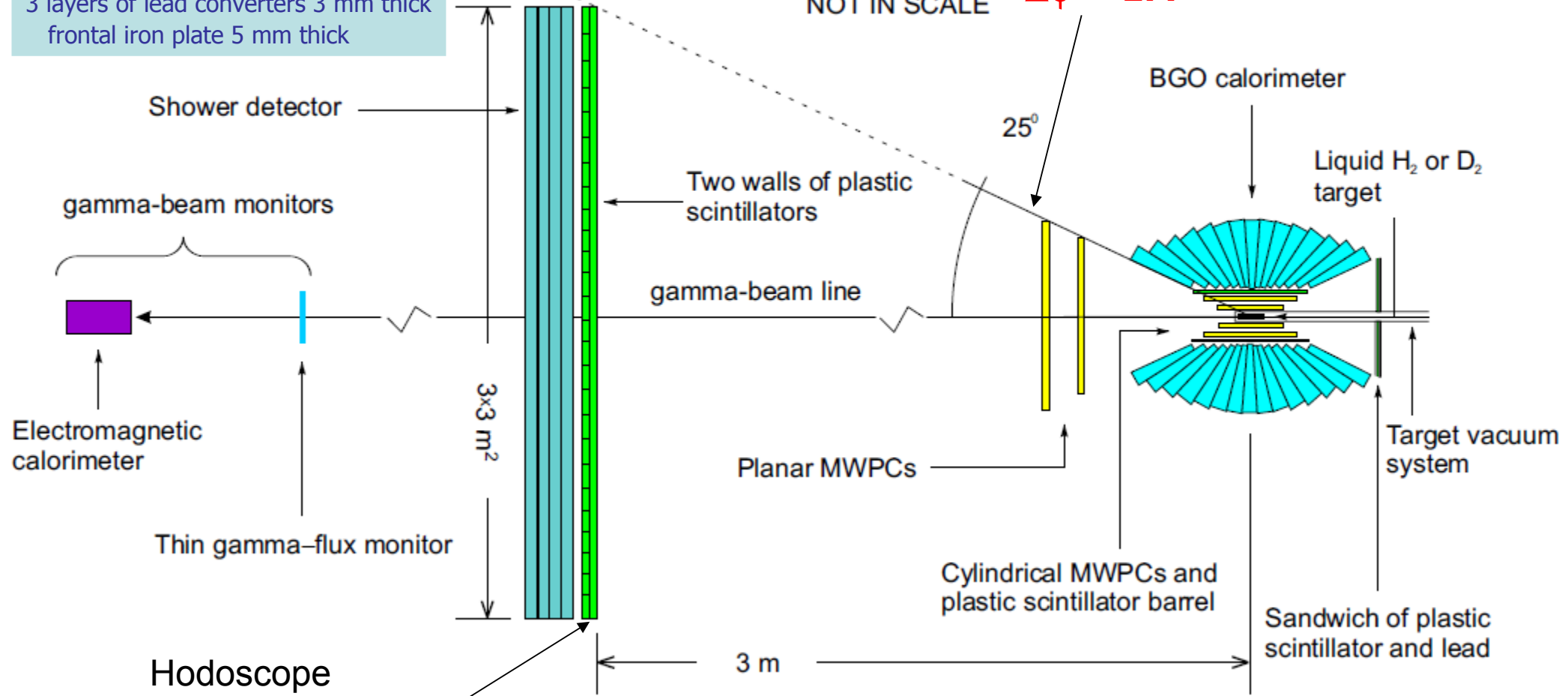


# Schematic view of the GRAAL detection system.

16 *sandwich* modules :  
 4 layers of scintillators 10 cm thick  
 3 layers of lead converters 3 mm thick  
 frontal iron plate 5 mm thick

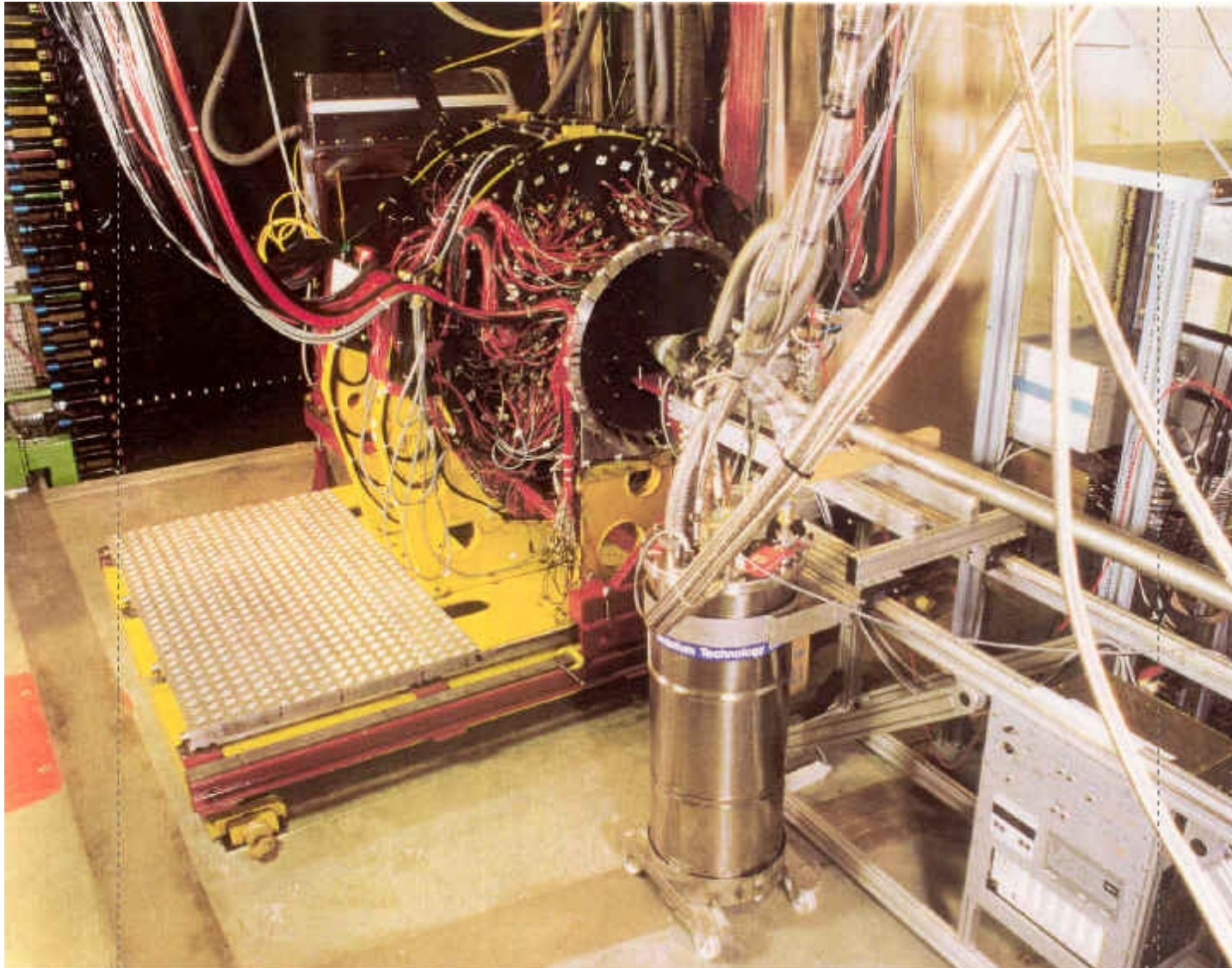
$\Delta \theta = 2^\circ$   
 $\Delta \phi = 1.4^\circ$

NOT IN SCALE



26 x 26 bars  
 NE110A  
 300 x 11,5 x 3 cm

## THE GRAAL DETECTOR: LAGRAN $\gamma$ E



**Large Acceptance Graal Apparatus for Nuclear  $\gamma$  Experiments**

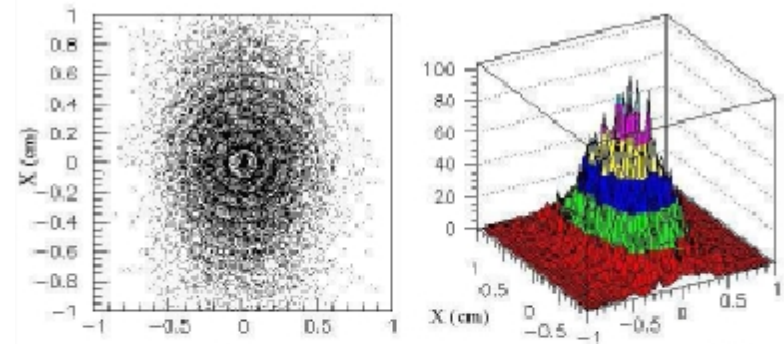
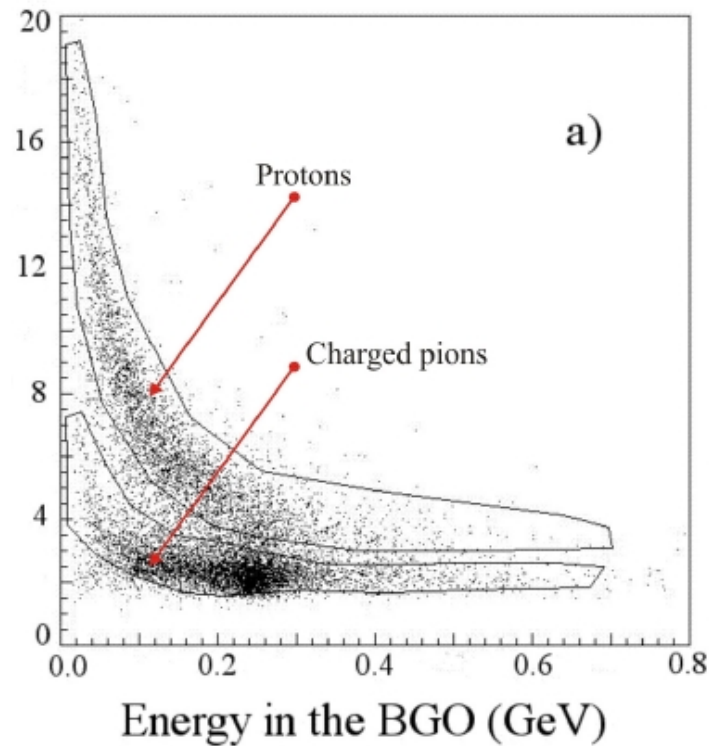
# Central detectors

**Pion/proton discrimination  
by means of  $dE/dx$  vs.  $E$**

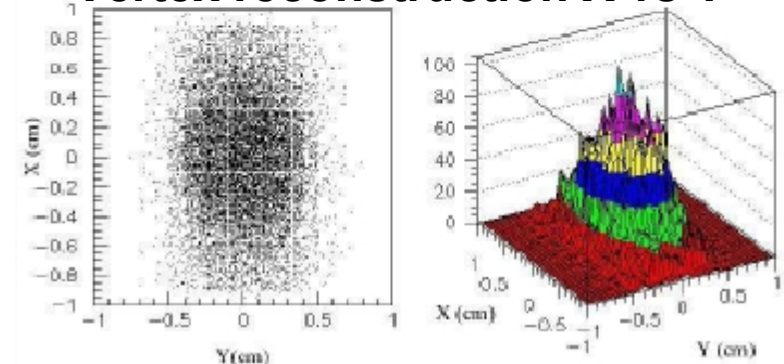
**Energy measurements for  
charge particles (protons)  
and photons**

Very good energy resolution  
for photons ( $\gamma$ ,  $\pi^0$ ,  $\eta$ ) and good  
response to protons up to 400 MeV

**DE/DX Barrell (MeV/cm)**

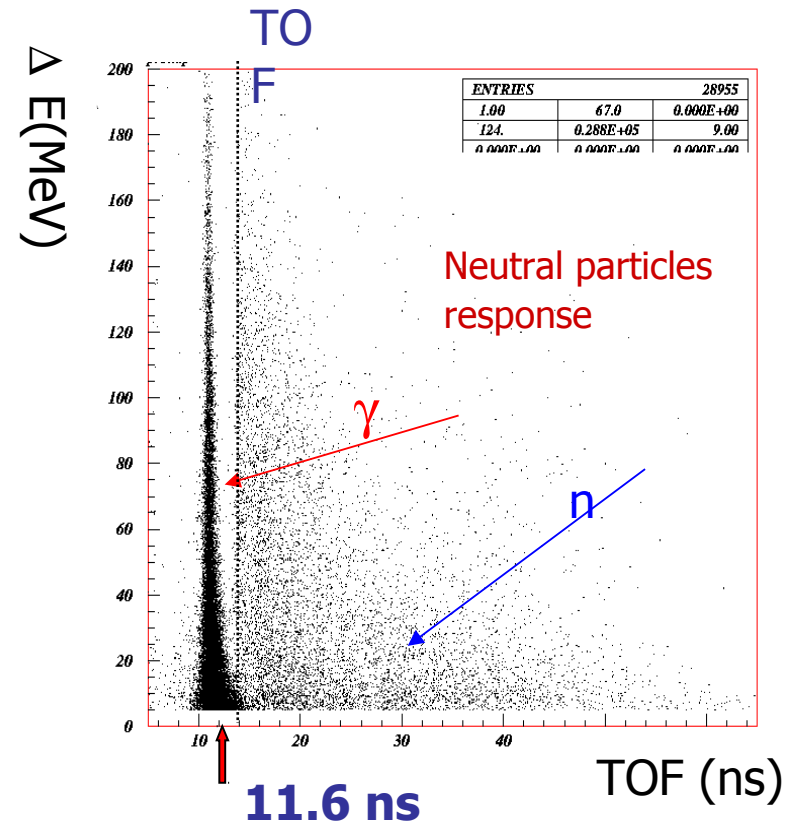
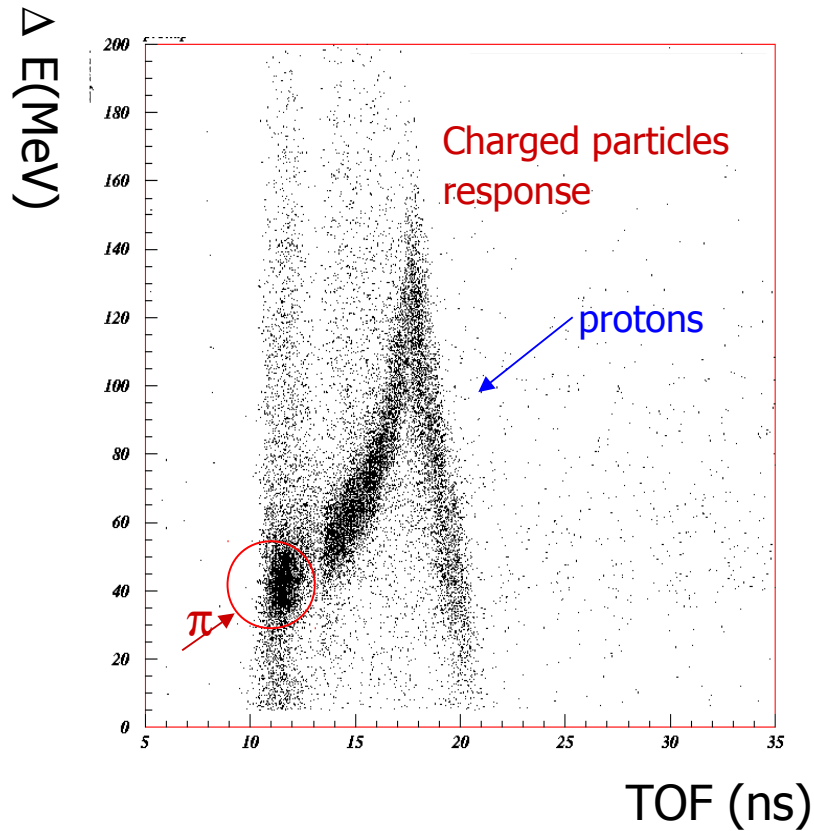


**Vertex reconstruction X vs Y**



# Forward Detectors

MWPC-P, Hodoscope wall, shower wall



Energy information for protons and neutrons

photon/neutron discrimination

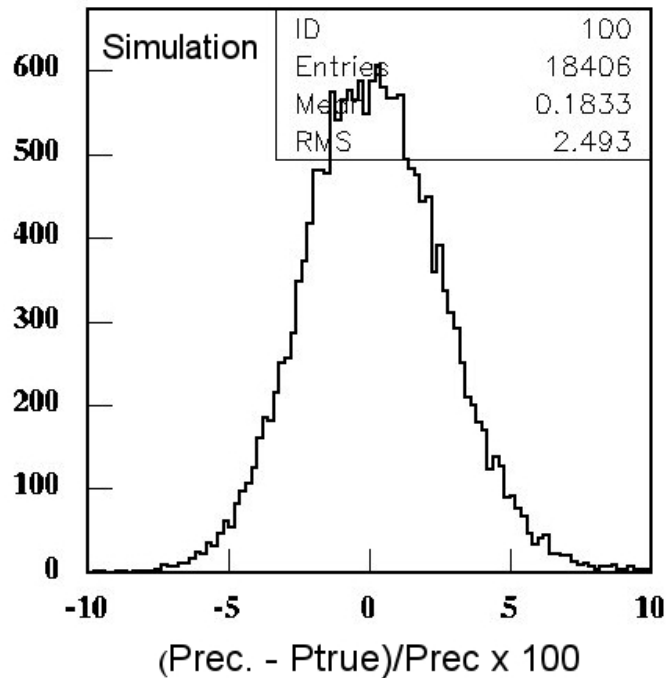
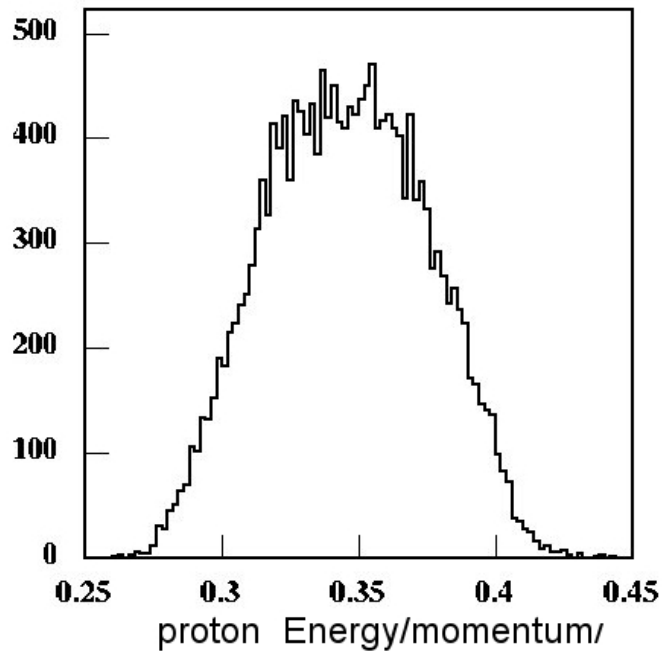
pion/proton discrimination

charged/neutral particle discrimination in coincidence with the hodoscope

# Missing mass to forward proton $M_p^{\text{miss}}$

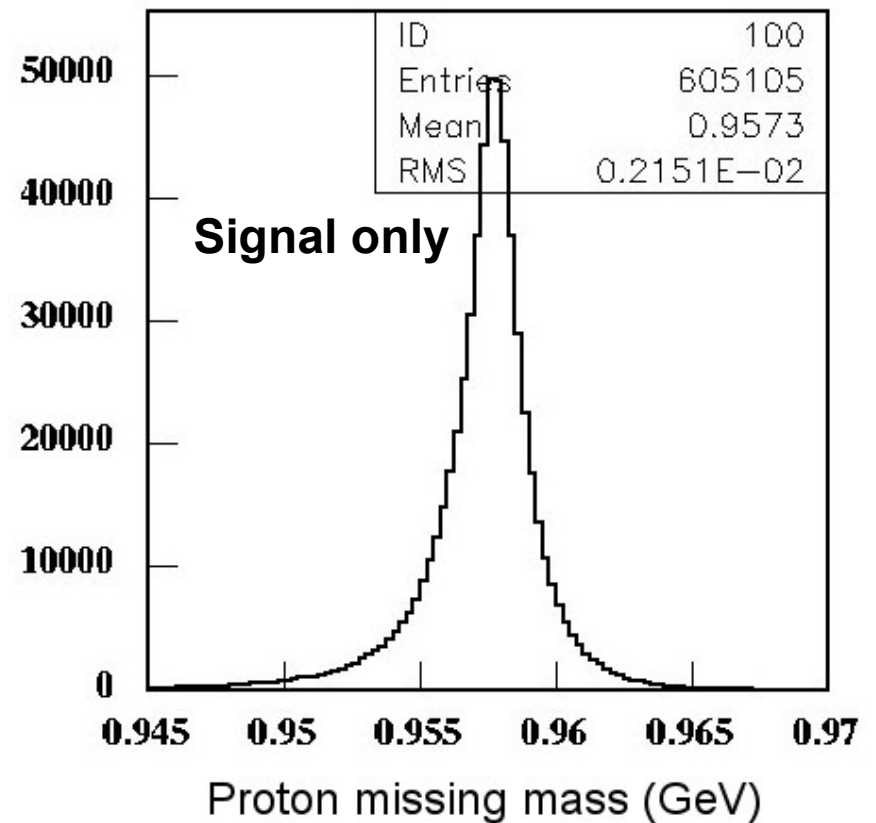
In the hypothesis of two body products in the final state reaction

$$\beta < 0.4$$

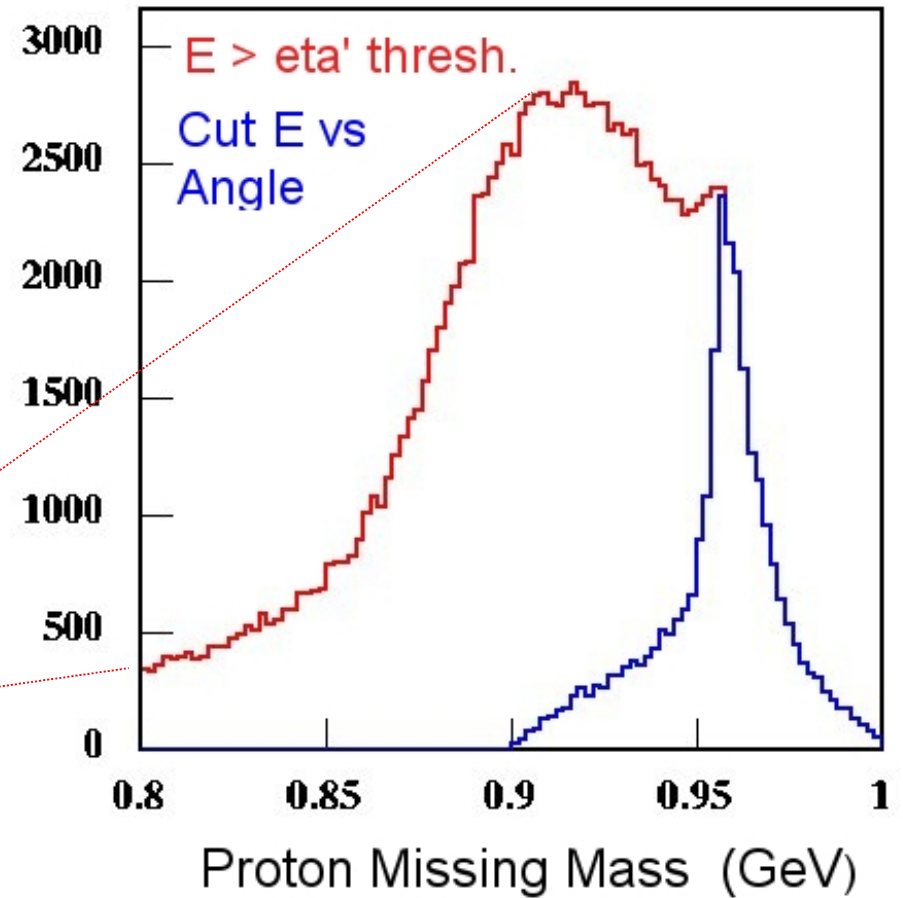
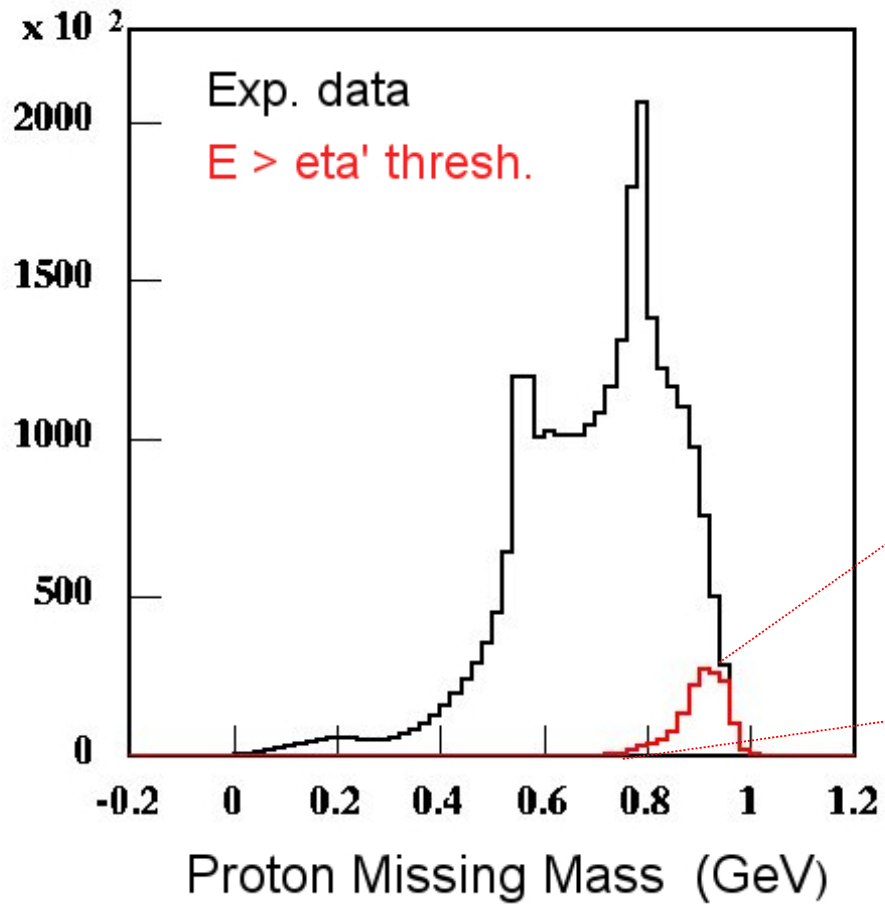


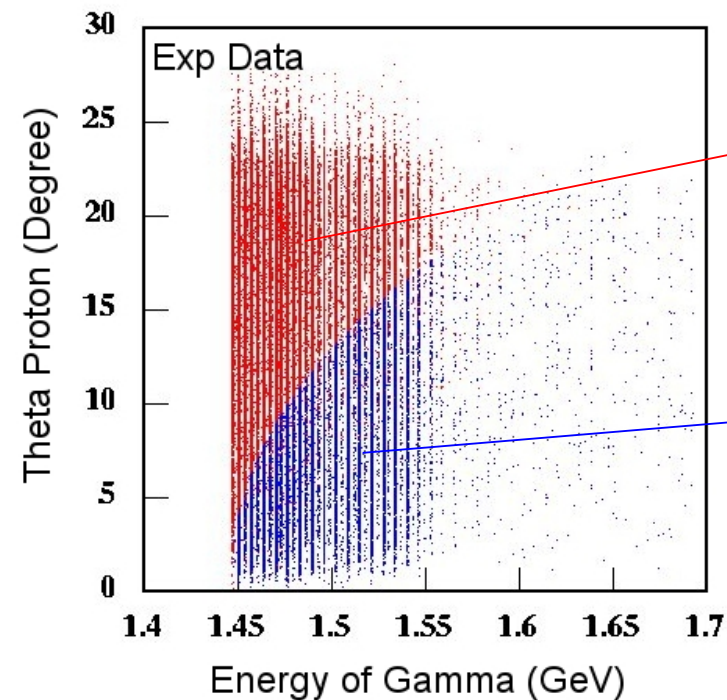
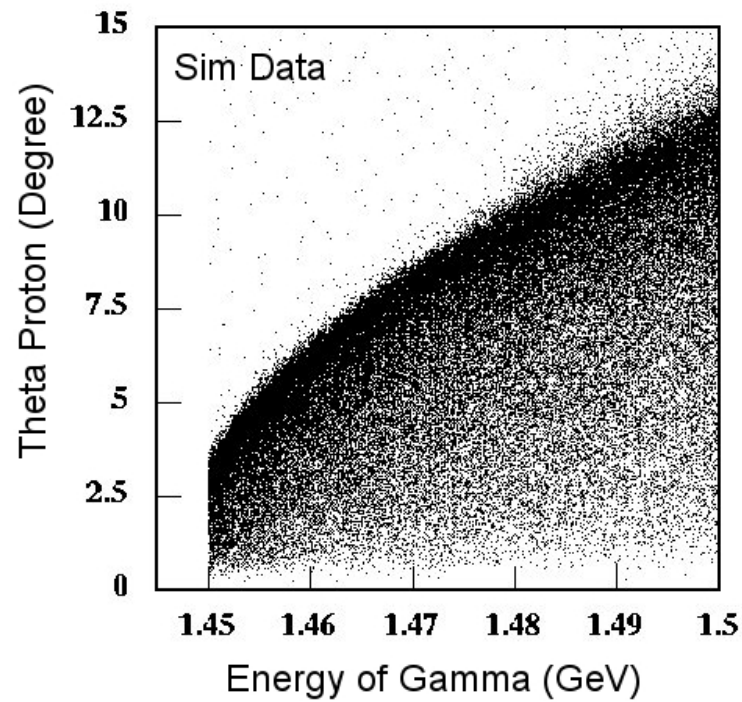
Momentum Resolution  
RMS = 2.5 %

RMS = 2.2 MeV

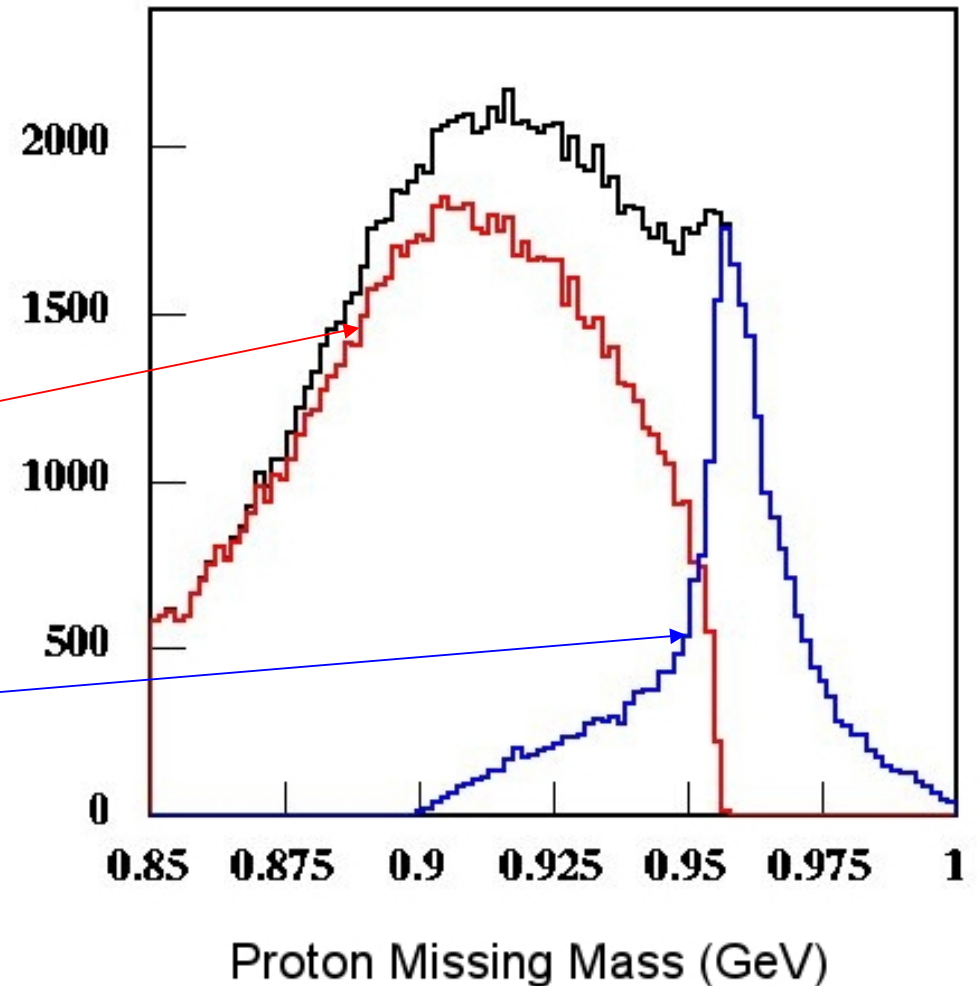


# Proton missing mass

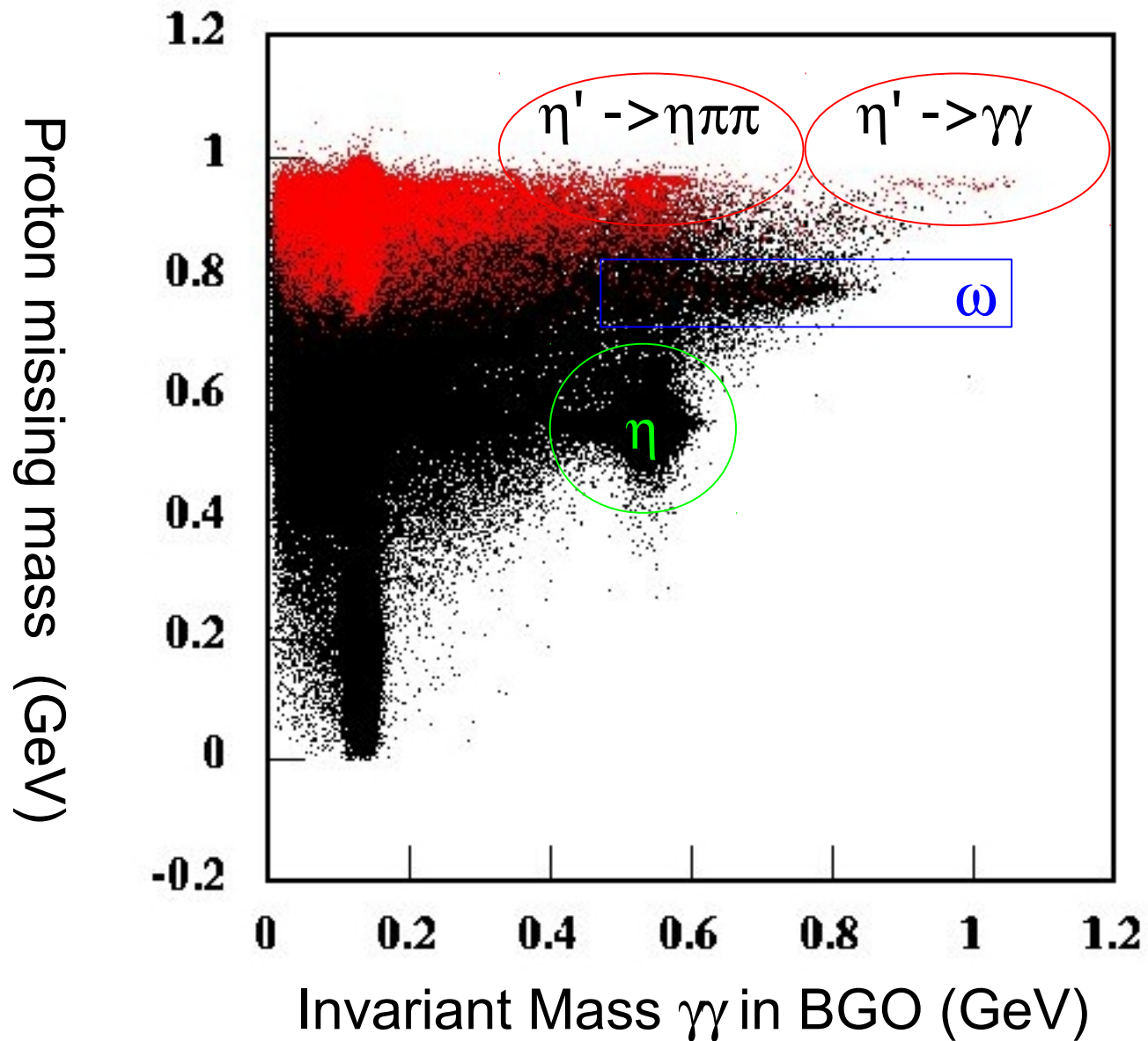




$E_{\gamma} - \theta_p$   
bidimensional cut

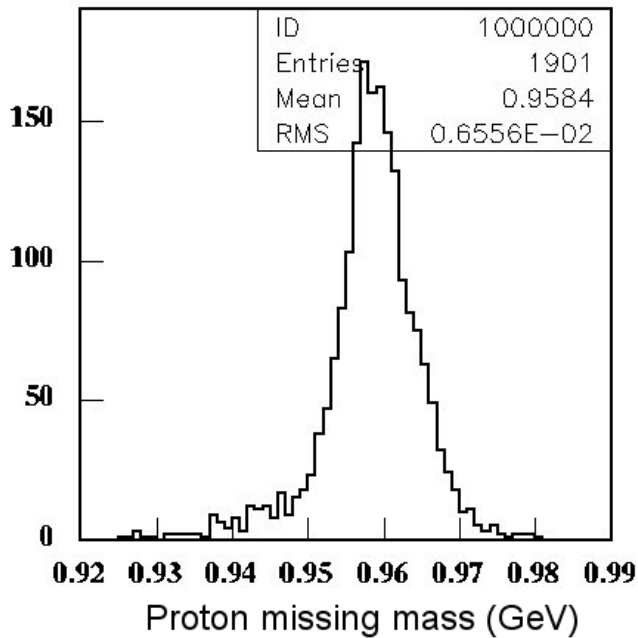


# $M_p^{\text{miss}}$ vs Inv. Mass $\gamma\gamma$ in BGO

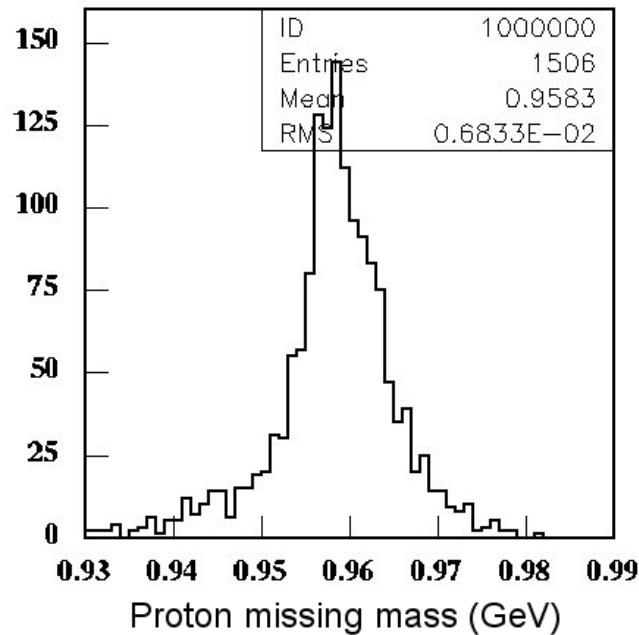


# Identified channels

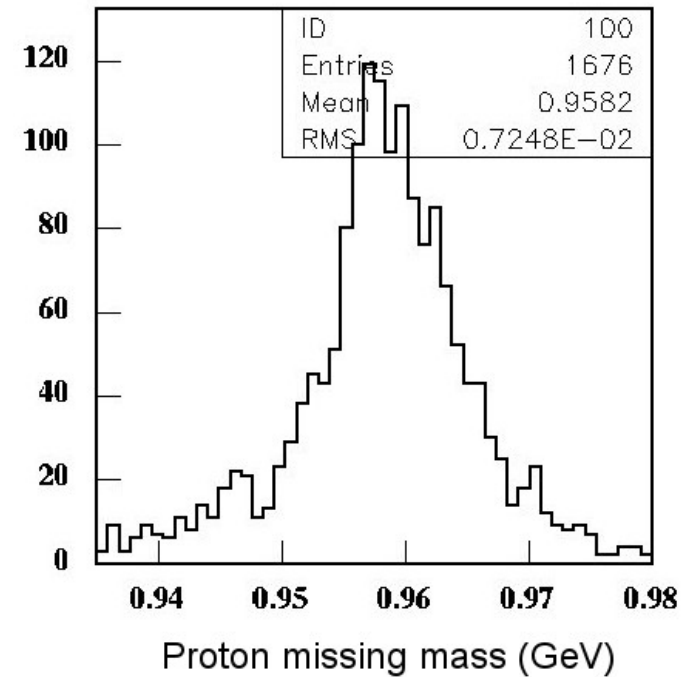
$\pi^+\pi^-\eta \rightarrow \pi^+\pi^-\gamma\gamma$



$\gamma\gamma$



$\pi^0\pi^0\eta$



We were able to identify different decay modes constraining the data with conditions on final state of  $h'$  particles decay

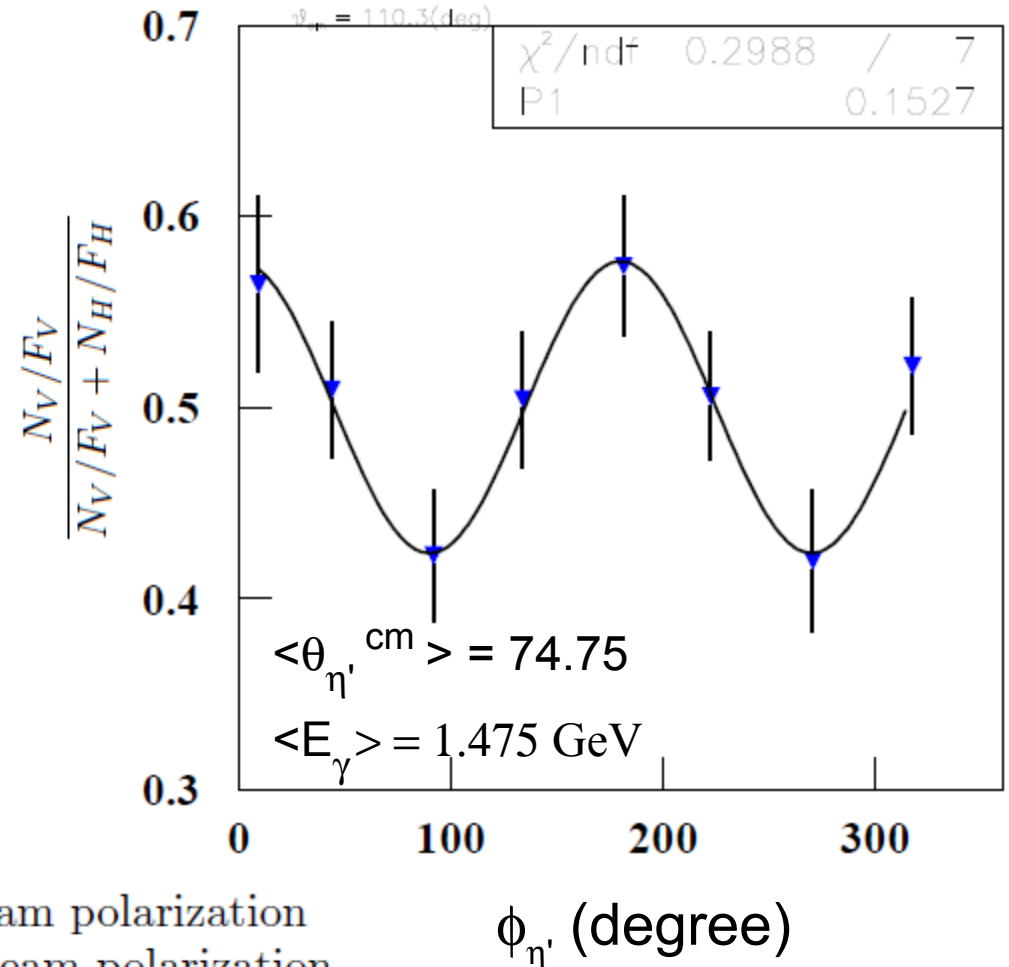
# Beam asymmetry extraction

Graal data on proton allow to cover with the present analysis the energy range up to 1.5 GeV (threshold = 1.446 GeV), with enough statistics to fit the  $P\Sigma$  distribution.

For each  $(E_\gamma, \theta_{\eta'}^{\text{cm}})$  fit of the azimuthal distribution of the ratio:

$$\frac{N_V/F_V}{N_V/F_V + N_H/F_H} = \frac{1}{2}[(1 + P\Sigma \cos(2\phi_{\eta'})]$$

- $N_{V,H}$  Events selected with vertical/horizontal beam polarization
- $F_{V,H}$  Flux corresponding to vertical/horizontal beam polarization
- $P$  Polarization degree of the beam at bin mean energy
- $\Sigma$  Beam asymmetry for every  $(E_\gamma, \theta_{\eta'}^{\text{cm}})$



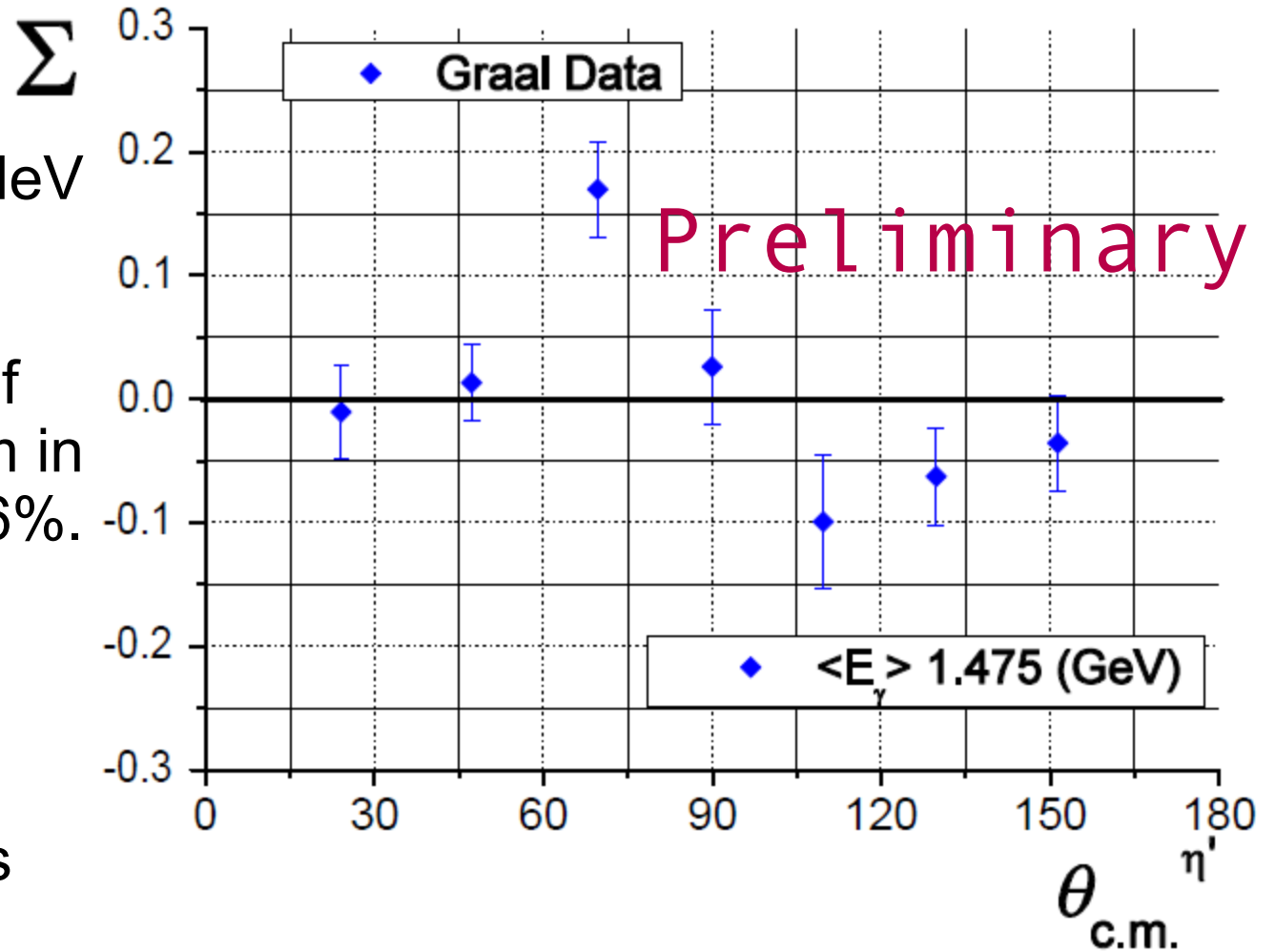
# Beam Asimmetry

We extracted 7 bin  
In theta cm of eta'  
In the energy bin: 45 MeV  
just over the threshold

The averaged degree of  
polarization of the beam in  
the considered bin is 96%.

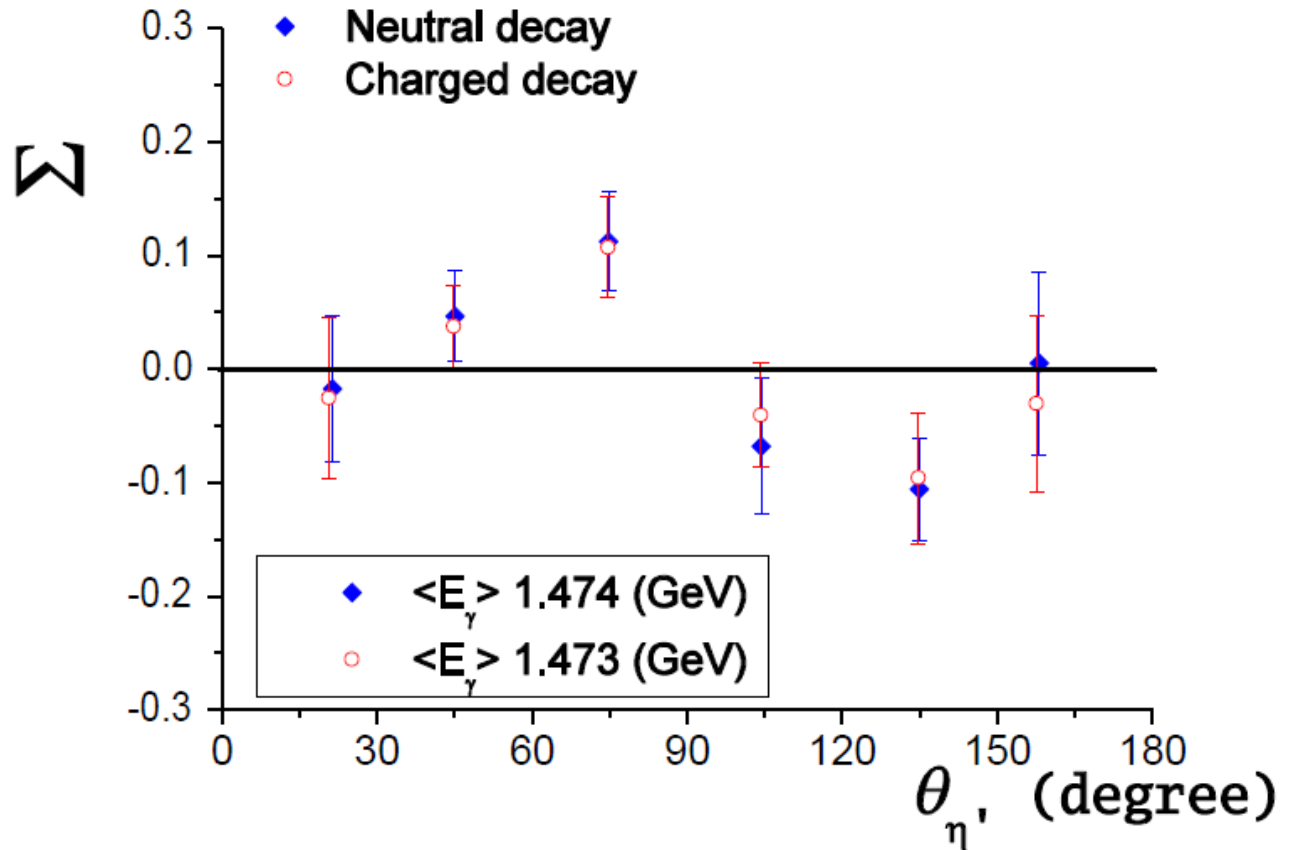
The results show the  
possible precence of  
S(1535) and P(1710)  
nucleon resonances as  
suggested in :

PRL 96, 062001 (2006)



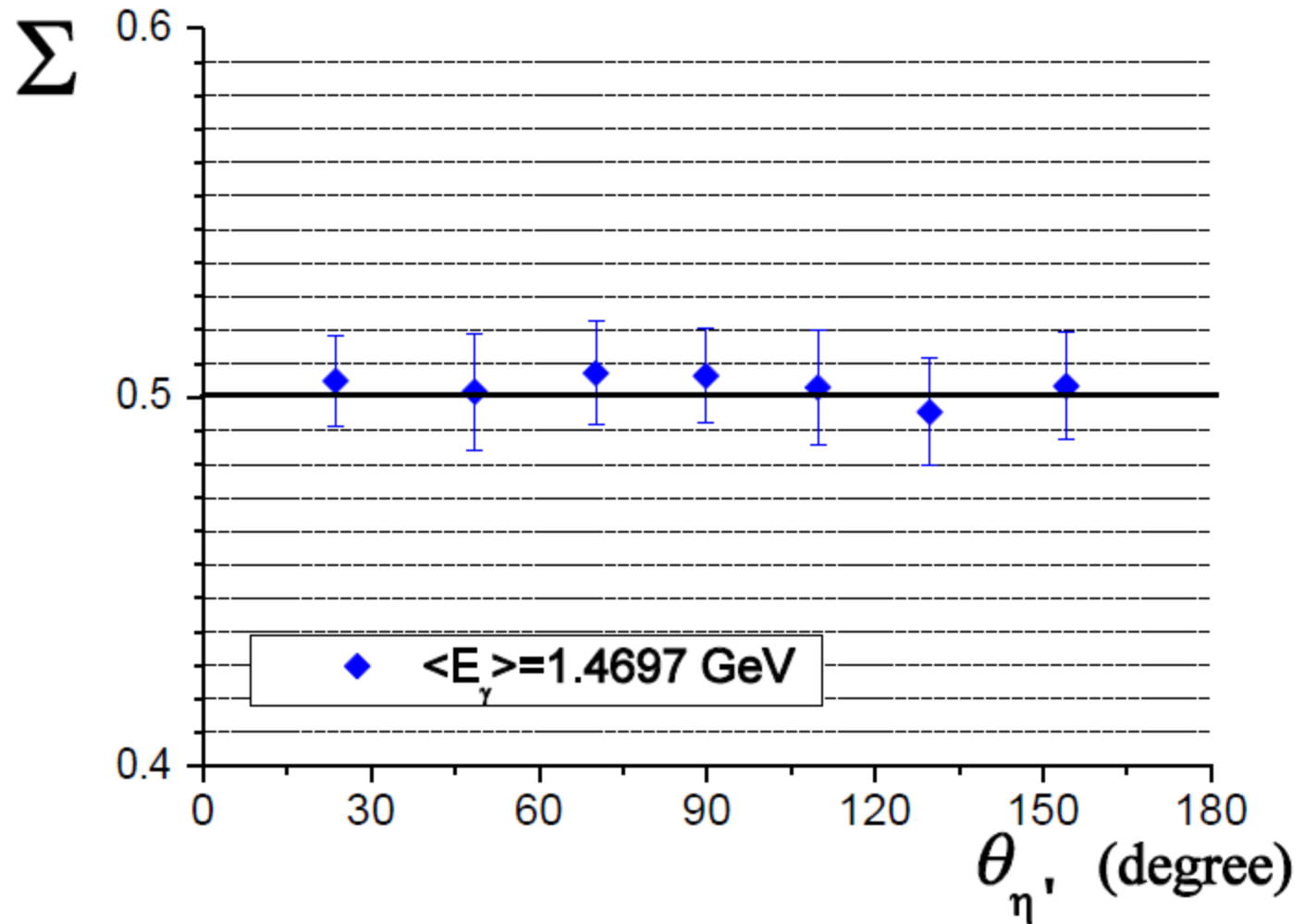
# Beam Asimmetry check

The comparison between beam asymmetry coming from the two independent samples of eta' events obtained from neutral decay particles only and from the charged decay particles are in good agreement.



# Beam Asimmetry check

A simulated sample with flat asymmetry equal to 0.5 was used to check the data analysis procedure used with experimental data. The extracted beam asymmetries are equal to  $0.5 \pm 0.01$ . The analysis software chain gives an uncertainty of  $\sim 1\%$ .



# Conclusion

All Graal data were analyzed to extract the beam asymmetry of  $\eta'$  photoproduction on free proton

The preliminary results of beam asymmetry were presented and checked with different tests, other checks are in progress.

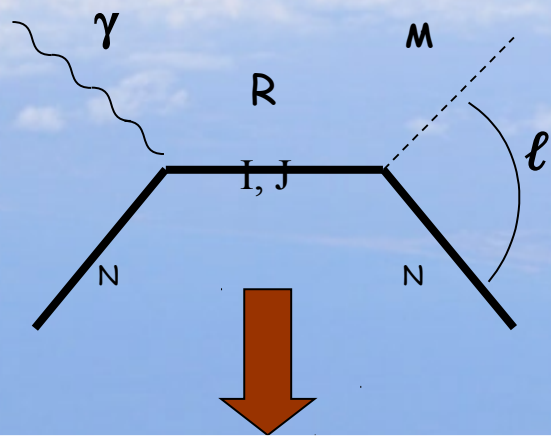
The results look like interesting considering the well controlled beam polarization degree.

Interpretation of results are in progress

In the near future we can expect new data for beam asymmetries from BGO-OD ELSA , CB-ELSA , CLAS experiments in a wide energy range.

SPARES

$$\ell_{212J}$$



**Open problems:**

- missing resonances"

$N^*$	Status	$SU(6) \otimes O(3)$	Parity	$\Delta^*$	Status	$SU(6) \otimes O(3)$
<b>I=1/2</b>				<b>I=3/2</b>		
P11(938)	****	(56,0 <sup>+</sup> )	+	P33(1232)	****	(56,0 <sup>+</sup> )
S11(1535)	****	(70,1 <sup>-</sup> )				
S11(1650)	****	(70,1 <sup>-</sup> )		S31(1620)	****	(70,1 <sup>-</sup> )
D13(1520)	****	(70,1 <sup>-</sup> )	-	D33(1700)	****	(70,1 <sup>-</sup> )
D13(1700)	***	(70,1 <sup>-</sup> )				
D15(1675)	****	(70,1 <sup>-</sup> )				
P11(1520)	****	(56,0 <sup>+</sup> )		P31(1875)	****	(56,2 <sup>+</sup> )
P11(1710)	***	(70,0 <sup>+</sup> )		P31(1835)		(70,0 <sup>+</sup> )
P11(1880)		(70,2 <sup>+</sup> )				
P11(1975)		(20,1 <sup>+</sup> )				
P13(1720)	****	(56,2 <sup>+</sup> )		P33(1600)	***	(56,0 <sup>+</sup> )
P13(1870)	*	(70,0 <sup>+</sup> )		P33(1920)	***	(56,2 <sup>+</sup> )
P13(1910)		(70,2 <sup>+</sup> )	+	P33(1985)		(70,2 <sup>+</sup> )
P13(1950)		(70,2 <sup>+</sup> )				
P13(2030)		(20,1 <sup>+</sup> )				
F15(1680)	****	(56,2 <sup>+</sup> )		F35(1905)	****	(56,2 <sup>+</sup> )
F15(2000)	**	(70,2 <sup>+</sup> )		F35(2000)	**	(70,2 <sup>+</sup> )
F15(1995)		(70,2 <sup>+</sup> )				
F17(1990)	**	(70,2 <sup>+</sup> )		F37(1950)	****	(56,2 <sup>+</sup> )

## DAL PUNTO DI VISTA SPERIMENTALE

Problema: il canale di decadimento dominante delle risonanze nucleoniche è il decadimento forte con emissione di uno o più mesoni

vite medie brevissime ( $\tau \approx 10^{-24}$  s)



**gli stati eccitati hanno**

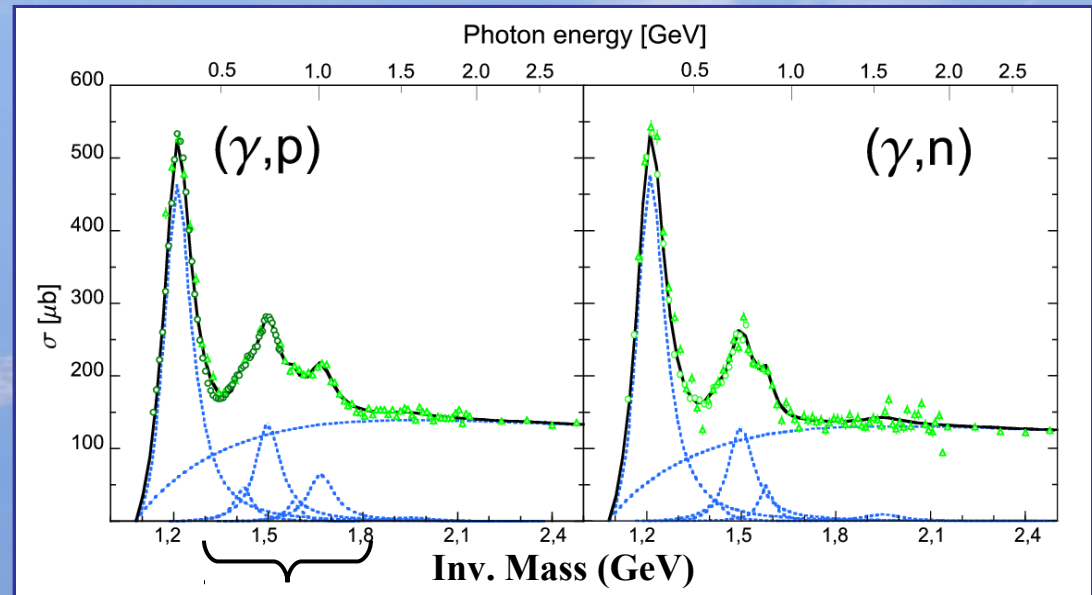


grandi larghezze (centinaio di MeV)



**forte sovrapposizione tra le curve delle varie risonanze**

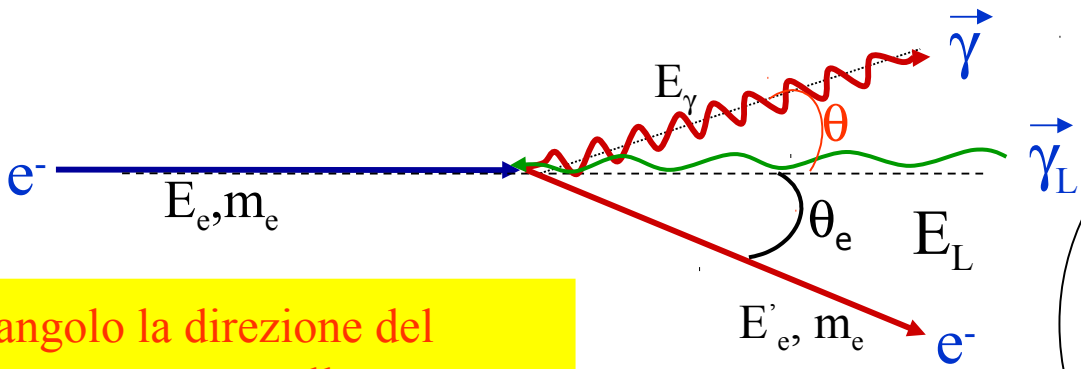
**Total photoabsorption cross section on proton/neutron**



**Second resonance region:  $P_{11}(1440)$ ,  $D_{13}(1520)$ ,  $S_{11}(1535)$**

Misure inclusive di fotoproduzione non permettono la separazione degli stati risonanti.

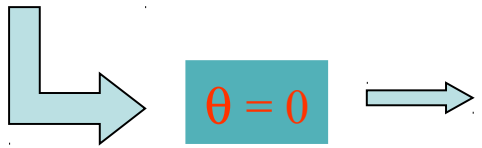
# PROCESSO DI BACKSCATTERING COMPTON



$\theta$  = angolo la direzione del fotone uscente e quella dell'elettrone incidente

$$E_\gamma = \frac{4 \gamma_e^2 E_L}{1 + (\gamma_e \theta)^2 + 4 \gamma_e E_L / m_e}$$

Energia del fotone uscente



$$E_\gamma^{\max} = \frac{4 \gamma_e^2 E_L}{1 + 4 \gamma_e E_L / m_e}$$

$E_e = 6.04 \text{ GeV}$

$E_L = 2.41 \text{ eV}$  (green line,  $\lambda = 514 \text{ nm}$ )

$E_L = 3.53 \text{ eV}$  (U.V. line,  $\lambda = 351 \text{ nm}$ )



$E_\gamma^{\max} = 1.1 \text{ GeV}$

$E_\gamma^{\max} = 1.5 \text{ GeV}$

$\gamma_e = \frac{E_e}{m_e} = 11820$

$\theta_e \approx 0^\circ$        $\beta_e \approx 1$

$\theta \approx 1/\gamma_e \approx 0^\circ$

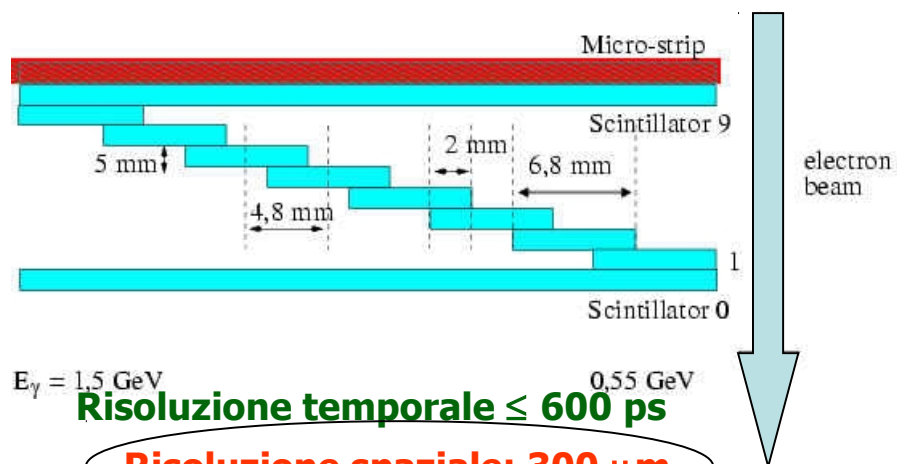
ESRF value

# Risoluzione energetica AND ENERGY SPECTRUM

## Sistema di tagging del fascio $\gamma$



**128  $\mu$ strip silicon detector + 10 fast plastic scintillators**, posizionati all'interno dello storage ring dietro il primo dipolo dopo la regione d'iterazione



**Risoluzione temporale  $\leq 600$  ps**

**Risoluzione spaziale:  $300 \mu\text{m}$**

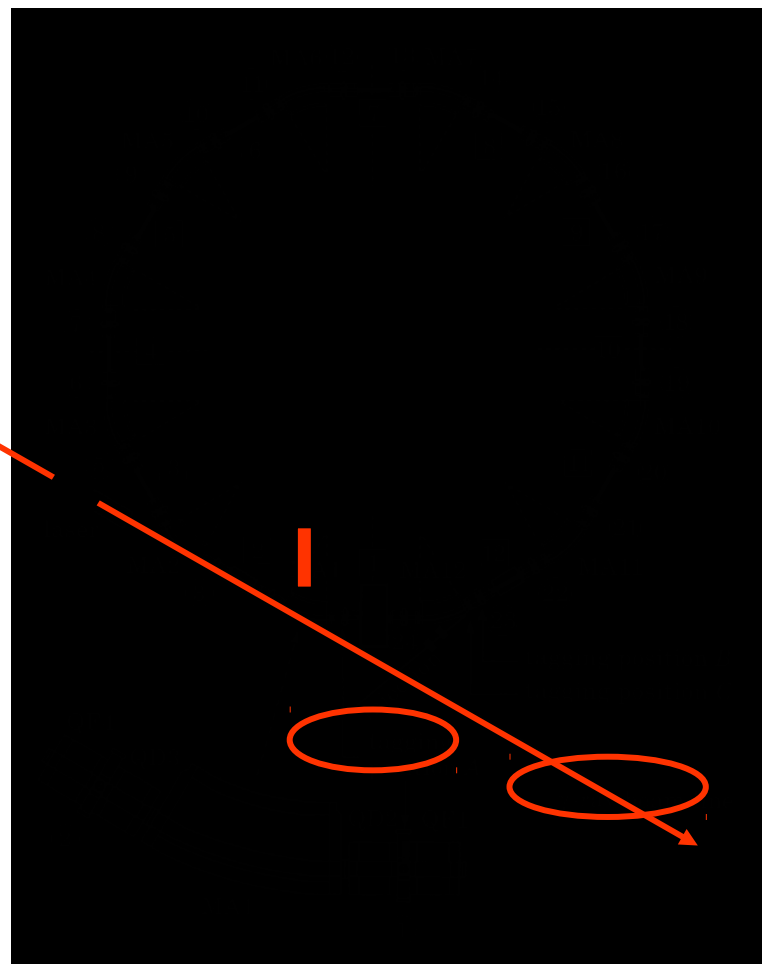
Misura dello scostamento dall'orbita originale degli elettroni d'uscita, a causa del passaggio attraverso il dipolo



$E_{e'}$

$$E_{\gamma} = E_e - E_{e'}$$

$$E_e + E_L = E_{e'} + E_{\gamma}$$



## ENERGY RESOLUTION AND ENERGY SPECTRUM (2)

Il tagging garantisce una risoluzione di **16 MeV (FWHM) (1.1%)**

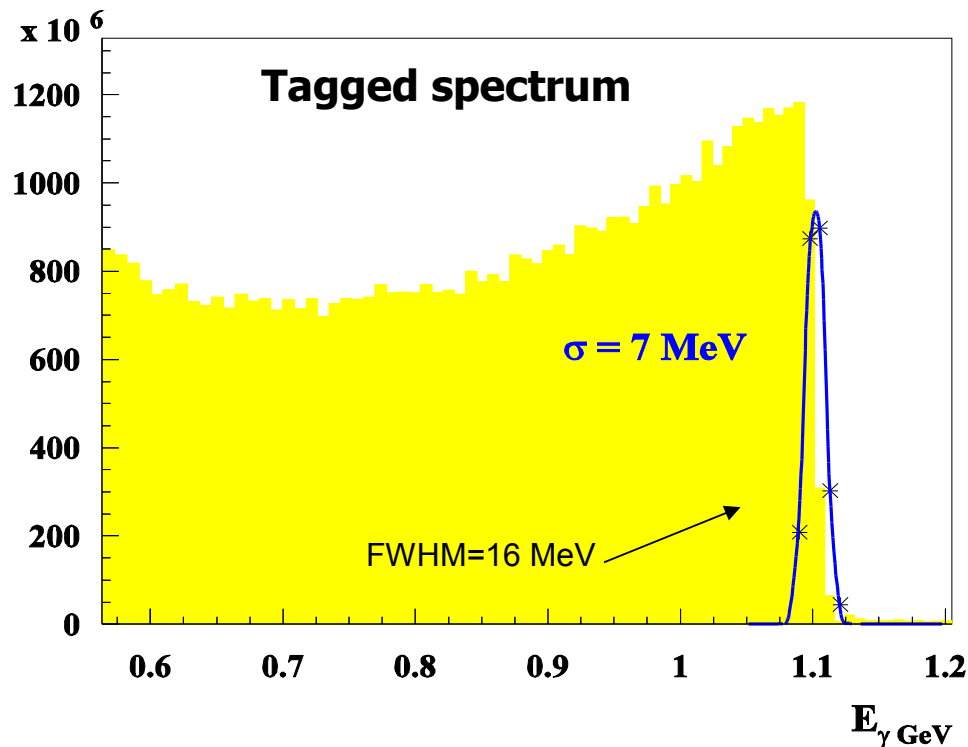
Il contributo principale alla risoluzione in energia è dovuto alla dispersione energetica del fascio di elettroni (14 MeV FWHM).

La sezione d'urto di backscattering ha una debole dipendenza dall'energia del gamma



Lo spettro di energia non presenta la crescita esponenziale alle basse energie tipica dei fasci di bremsstrahlung ( $\sigma_{\text{brem}}(k_\gamma) \propto 1/k_\gamma$ )

Il fondo nel fascio di tagging è dovuto solo ai **Bremsstrahlung  $\gamma$ -rays** prodotti dal fascio di elettroni nel gas residuo della camera da vuoto.



$$\frac{dn}{dt} \text{background} \approx 5 \cdot 10^{-3} \frac{dn}{dt} \text{beam}$$

# γ BEAM POLARIZATION

- polarized laser beam ( $P_L=100\%$ )
- relativistic electrons: helicity is a good quantum number

Il grado di polarizzazione **non** può essere ridotta dal electron spin-flip

The only "polarization loss" is associated to the relative angular momentum  $\ell$  between the electron and the outgoing photon

the produced  $\gamma$  beam is polarized as a function of the out-going photon energy.

$$E_\gamma = \frac{4 \gamma_e^2 E_L}{1 + (\gamma_e \theta)^2 + 4 \gamma_e E_L / m_e}$$

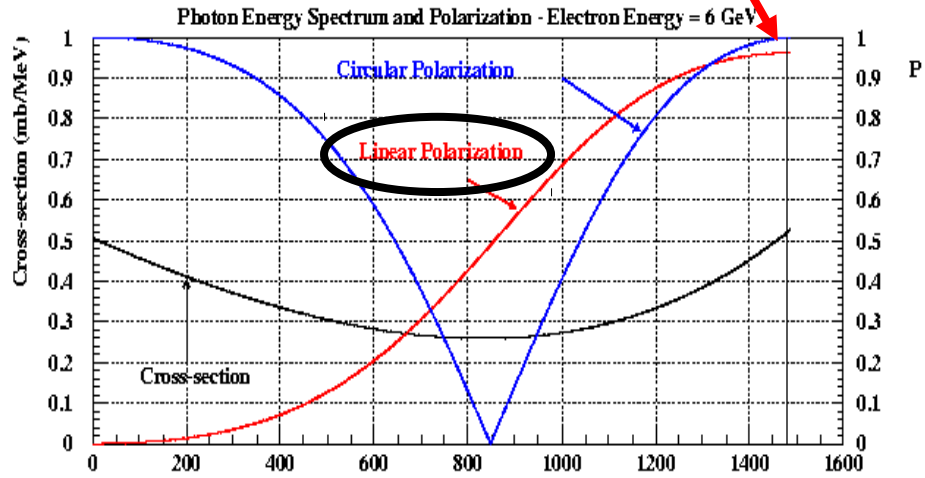
The polarization degree of the  $\gamma$  beam depends on the  $\theta$  angle of the outgoing photon

Compton Backscattering is an electromagnetic interaction

$\theta = 0 \Rightarrow \ell = 0$   
 $E_\gamma = E_\gamma^{\max} \Rightarrow P_\gamma \approx 100\%$

perturbative QED calculation

**Polarization degree of the  $\vec{\gamma}$  beam as function of the  $P_L$  and the  $E_\gamma$**



## $\gamma$ BEAM POLARIZATION (2)

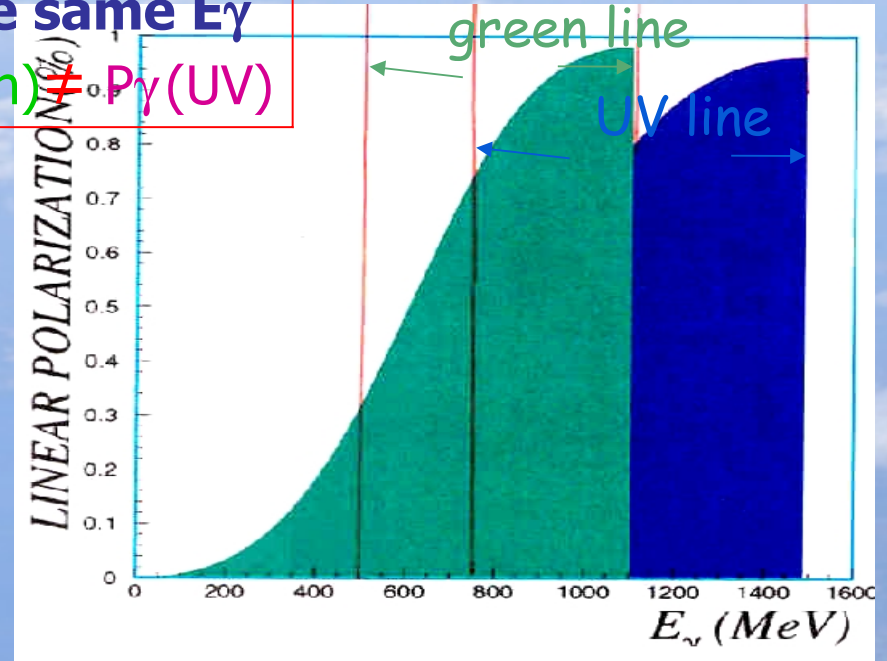
Two different laser lines: UV, green

$$E_{\gamma}^{\max}(\text{green}) \neq E_{\gamma}^{\max}(\text{UV})$$

$$\text{For the same } E_{\gamma} \\ P_{\gamma}(\text{green}) \neq P_{\gamma}(\text{UV})$$

It is possible to study a given reaction at the same energy but with different polarization values.

**Strong cross check of the data**



The laser photon transfers its polarization to the  $\gamma$ -ray

The polarization direction of the  $\gamma$  beam can be changed simply changing the laser polarization

Acquisition of data with different polarization directions during the same run

**same experimental condition => reduction of systematic errors**